Article

Chemical Shift Anisotropy Tensors of Carbonyl, Nitrogen, and Amide Proton Nuclei in Proteins through Cross-Correlated Relaxation in NMR Spectroscopy

Karine Loth, Philippe Pelupessy, and Geoffrey Bodenhausen

J. Am. Chem. Soc., **2005**, 127 (16), 6062-6068• DOI: 10.1021/ja042863o • Publication Date (Web): 02 April 2005

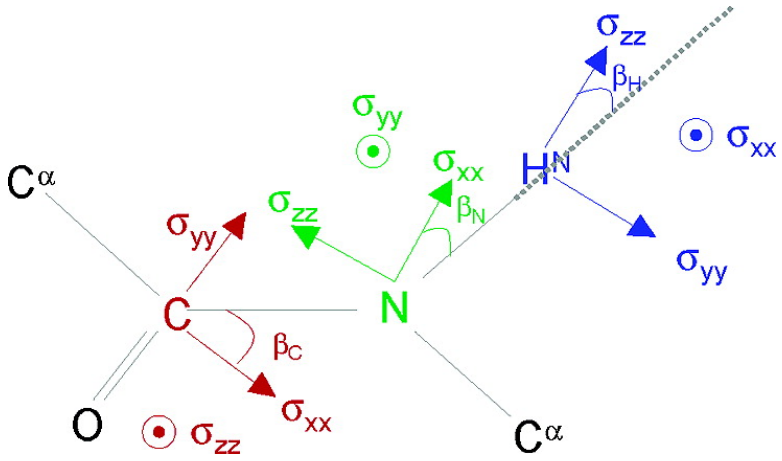

More About This Article

Additional resources and features associated with this article are available within the HTML version:

- Supporting Information
- Links to the 9 articles that cite this article, as of the time of this article download
- Access to high resolution figures
- Links to articles and content related to this article
- Copyright permission to reproduce figures and/or text from this article

View the Full Text HTML

J|A|C|S
ARTICLES
Published on Web 04/02/2005

Chemical Shift Anisotropy Tensors of Carbonyl, Nitrogen, and Amide Proton Nuclei in Proteins through Cross-Correlated Relaxation in NMR Spectroscopy

Karine Loth,[†] Philippe Pelupessy,*[,†,‡] and Geoffrey Bodenhausen[†,‡]

Contribution from the Département de Chimie, Associé au CNRS, Ecole Normale Supérieure, 24 rue Lhomond, 75231 Paris Cedex 05, France, and Institut des Sciences et Ingénierie Chimiques, Ecole Polytechnique Fédérale de Lausanne, BCH, 1015 Lausanne, Switzerland

Received November 26, 2004; E-mail: philippe.pelupessy@ens.fr

Abstract: The principal components and orientations of the chemical shift anisotropy (CSA) tensors of the carbonyl (C′), nitrogen (N), and amide proton (H^N) nuclei of 64 distinct amide bonds in human ubiquitin have been determined in isotropic solution by a set of 14 complementary auto- and cross-correlated relaxation rates involving the CSA interactions of the nuclei of interest and several dipole−dipole (DD) interactions. The CSA parameters thus obtained depend to some degree on the models used for local motions. Three cases have been considered: restricted isotropic diffusion, three-dimensional Gaussian axial fluctuations (3D-GAF), and independent out-of-plane motions of the NH^N vectors with respect to the peptide planes.

Introduction

A chemical shift anisotropy (CSA) tensor can be described by three principal components and three Euler angles, which describe its orientation with respect to the molecular frame. In many systems of interest, one of the principal axes lies perpendicular to a local plane of symmetry, so that only one angle suffices to determine the positions of the remaining two principal axes with respect to the molecular frame. Furthermore, the sum of the three components is usually known, so that there are only three independent parameters that need to be determined for each tensor.

Accurate knowledge of CSA tensors is important for many solid-state NMR studies.[1,2] For example, CSA interactions of carbonyl nuclei in peptides can be correlated with $C^\alpha H^\alpha$ dipolar couplings[3] or with CSA interactions of other carbonyl nuclei[4] in so-called separated-local-field double quantum experiments to obtain information about backbone dihedral angles. CSA parameters are needed to simulate the yield of magnetization transfer under rotational resonance in magic angle spinning (MAS) to determine internuclear distances.[5] The interpretation of PISEMA spectra[6] of membrane proteins embedded in oriented lipid bilayers depends on the orientation of nitrogen CSA tensors with respect to nitrogen−proton bonds.

Precise information about CSA parameters is also needed to validate quantum-chemical calculations[7−9] and to exploit relaxation rates[10,11] and residual anisotropic chemical shifts in liquid-state NMR.[12−14] Thus, dihedral angles can be obtained by measurements of CSA/dipole−dipole or CSA/CSA cross-correlation rates in biomolecules such as proteins[15−18] or RNA.[19,20] Correlated variations of isotropic chemical shifts of two nuclei due to slow motions[21−23] have the same effect as CSA/CSA cross-correlated relaxation and can only be quantified if the CSA parameters are known.

In solid-state NMR, CSA tensors can be determined from single-crystal spectra,[24] powder patterns,[25,26] or MAS spectra.[27,28]

[†] Ecole Normale Supérieure.
[‡] Ecole Polytechnique Fédérale de Lausanne.

(1) Weliky, D. P.; Tycko, R. *J. Am. Chem. Soc.* **1996**, *118*, 8487−8488.
(2) Opella, S. J.; Marassi, F. *Chem. Rev.* **2004**, *104*, 3587−3606.
(3) Schmidt-Rohr, K. *J. Am. Chem. Soc.* **1996**, *118*, 7601−7603.
(4) Blanco, F. J.; Tycko, R. *J. Magn. Reson.* **2001**, *149*, 131−138.
(5) Raleigh, D. P.; Creuzet, F.; Das Gupta, S. K.; Levitt, M. H.; Griffin, R. G. *J. Am. Chem. Soc.* **1989**, *111*, 4502−4503.
(6) Wu, C. H.; Ramamoorthy, A.; Opella, S. J. *J. Magn. Reson., Ser. A* **1994**, *109*, 270−272.
(7) de Dios, A. C.; Pearson, J. G.; Oldfield, E. *Science* **1993**, *260*, 1491−1496.
(8) Facelli, J. C.; Grant, D. M. *Nature* **1993**, *365*, 325−327.
(9) de Dios, A. C.; Oldfield, E. *J. Am. Chem. Soc.* **1994**, *116*, 11485−11488.
(10) Schwalbe, H.; Carlomagno, T.; Hennig, M.; Junker, J.; Reif, B.; Richter, C.; Griesinger, C. *Methods Enzymol.* **2001**, *338*, 35−81.
(11) Frueh, D. *Prog. Nucl. Magn. Reson. Spectrosc.* **2002**, *41*, 305−324.
(12) Boyd, J.; Redfield, C. *J. Am. Chem. Soc.* **1999**, *121*, 7441−7442.
(13) Cornilescu, G.; Bax, A. *J. Am. Chem. Soc.* **2000**, *122*, 10143−10154.
(14) Lipsitz, R.; Tjandra, N. *J. Magn. Reson.* **2003**, *164*, 171−176.
(15) Yang, D.; Konrat, R.; Kay, L. E. *J. Am. Chem. Soc.* **1997**, *119*, 11938−11940.
(16) Chiarparin, E.; Pelupessy, P.; Ghose, R.; Bodenhausen, G. *J. Am. Chem. Soc.* **1999**, *121*, 6876−6883.
(17) Skrynnikov, N. R.; Konrat, R.; Muhandiram, D. R.; Kay, L. E. *J. Am. Chem. Soc.* **2000**, *122*, 7059−7071.
(18) Kloiber, K.; Schuler, W.; Konrat, R. *J. Biomol. NMR* **2002**, *22*, 349−363.
(19) Ravindranathan, S.; Kim, C.-H.; Bodenhausen, G. *J. Biomol. NMR* **2003**, *27*, 365−375.
(20) Duchardt, E.; Richter, C.; Ohlenschlager, O.; Gorlach, M.; Wohnert, J.; Schwalbe, H. *J. Am. Chem. Soc.* **2004**, *126*, 1962−1970.
(21) Schuler, W.; Kloiber, K.; Matt, T.; Bister, K.; Konrat, R. *Biochemistry* **2001**, *40*, 9596−9604.
(22) Frueh, D.; Tolman, J. R.; Bodenhausen, G.; Zwahlen, C. *J. Am. Chem. Soc.* **2001**, *123*, 4810−4813.
(23) Wist, J.; Frueh, D.; Tolman, J. L.; Bodenhausen, G. *J. Biomol. NMR* **2004**, *28*, 263−272.
(24) Pausak, S.; Pines, A.; Waugh, J. S. *J. Chem. Phys.* **1973**, *59*, 591−595.
(25) Kaplan, S.; Pines, A.; Griffin, R. G.; Waugh, J. S. *Chem. Phys. Lett.* **1974**, *25*, 78−79.
(26) Linder, M.; Höhener, A.; Ernst, R. R. *J. Chem. Phys.* **1980**, *73*, 4959−4970.
(27) Stejskal, E. O.; Schaefer, J.; McKay, R. A. *J. Magn. Reson.* **1977**, *25*, 569−573.

10.1021/ja042863o CCC: $30.25

However, these methods only allow one to study a limited number of nuclei. When a molecule is partially oriented (which can be achieved in anisotropic media or by paramagnetic effects), one can observe residual anisotropic chemical shifts.[12,29] In isotropic solution, one observes only the isotropic chemical shift, $\sigma_{iso} = (\sigma_{xx} + \sigma_{yy} + \sigma_{zz})/3$, that is, the average of the principal components of the CSA tensor. However, the combination of various auto- and cross-correlated relaxation rates allows one to extract the full set of CSA parameters.

Several studies have focused on carbonyl CSA tensors of peptides in the solid phase.[30−35] In isotropic solution, Pang and Zuiderweg[36] determined the principal components and orientations of the CSA tensors of 71 carbonyl nuclei in the protein binase using a set of complementary cross-correlated relaxation rates. Cisnetti et al.[37] determined the CSA parameters of 63 carbonyl nuclei in ubiquitin with more elaborate techniques. Markwick and Sattler[38] calculated the CSA parameters of carbonyl nuclei using density functional theory and molecular dynamics and used cross-correlated relaxation rates to validate their approach. The latter two studies came to very similar conclusions: the variation of the isotropic chemical shifts of the carbonyl nuclei is largely determined by changes in the principal component σ_{yy} that is almost parallel to the CO bond while the two other components σ_{xx} and σ_{zz} are relatively constant.

Nitrogen CSA tensors in peptides have also been extensively studied by solid-state NMR.[33,39−41] Fushman et al.[42,43] developed a "model independent" method to measure the anisotropy and orientation of CSA tensors by determining the ratio between the transverse CSA/DD cross-correlation rates, $R(N/NH^N)$, and the transverse auto-relaxation rate, $R_2(N)$, at different magnetic fields. This approach was later refined by Damberg et al., who included longitudinal cross- and auto-correlation rates in the analysis.[44] Several groups[45−47] considered the field dependence of auto-correlated relaxation rates $R_1(N)$ and $R_2(N)$. In the latter approaches, the CSA tensors were assumed to be axially symmetric. Note that no information about the orientation of CSA tensors can be extracted from auto-correlated relaxation rates.

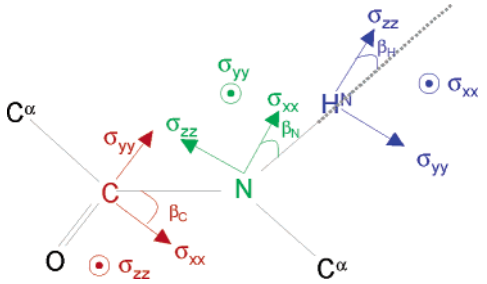

Figure 1. Local structure of a peptide plane in a protein. Ideally, all atoms lie in the same plane. The principal components and the orientation of the CSA tensors of the carbonyl (C′), nitrogen (N), and amide proton (H^N) are represented in red, green, and blue, respectively. The principal components of the CSA tensors are defined so that $\sigma_{zz} < \sigma_{yy} < \sigma_{xx}$ (i.e., σ_{zz} most and σ_{xx} least shielded) and $(\sigma_{zz} + \sigma_{yy} + \sigma_{xx})/3 = \sigma_{iso}$. One of the components lies perpendicular to the peptide plane, so that the orientation of each CSA tensor can be defined by one angle β.

Information on the CSA tensors of amide protons H^N in peptides and proteins is much scarcer. Only a few solid-state studies[48,49] and a few studies based on the transverse CSA/DD cross-correlation rate $R(H^N/H^NN)$ in solution[50−52] have been published. Cornilescu and Bax[13] determined average CSA parameters of amide proton, nitrogen, and carbonyl nuclei by using residual anisotropic chemical shifts (RACS). Although, in principle, one can obtain site-specific CSA parameters by measuring RACS in several oriented media, only average CSA parameters have been obtained thus far. In this work, we show that residue-specific CSA parameters of the amide proton H^N, nitrogen N, and carbonyl C′ nuclei can be obtained in solution state NMR by using a set of 14 complementary cross- and auto-correlated relaxation rates.

Theory

In Figure 1, the principal components of the CSA tensors of the ^{15}N, $^{13}C'$, and $^1H^N$ nuclei are shown. We assume that one of the principal components of each CSA tensor is perpendicular to the peptide plane. As a result, only one angle is required to define the orientation of each CSA tensor with respect to the molecular frame. The CSA/DD cross-correlation rate of a single quantum coherence I_y is given by:[53]

$$R(I/IS) = 2c_I c_{IS}\{(\sigma_{xx}^I - \sigma_{zz}^I)[4J_{xx,IS}(0) + 3J_{xx,IS}(\omega_I)] + (\sigma_{yy}^I - \sigma_{xx}^I)[4J_{yy,IS}(0) + 3J_{yy,IS}(\omega_I)]\} \quad (1)$$

where $c_{IS} = \mu_0\hbar\gamma_I\gamma_S\sqrt{2}/(16\pi r_{IS}^3)$ and $c_I = \omega_I\sqrt{2}/6$ with $\omega_I = -\gamma_I B_0$. The spectral densities $J(\omega)$ depend on the orientations of the DD interactions and principal components σ_{xx} and σ_{yy} of the CSA tensors and on motional parameters. The exact form

(28) Tycko, R.; Dabbagh, G.; Mirau, P. A. *J. Magn. Reson.* **1989**, *85*, 265−274.
(29) Ottiger, M.; Tjandra, N.; Bax, A. *J. Am. Chem. Soc.* **1997**, *119*, 9825−9830.
(30) Stark, R. E.; Jelinski, L. W.; Ruben, D. J.; Torchia, D. A.; Griffin, R. G. *J. Magn. Reson.* **1983**, *55*, 266−273.
(31) Oas, T. G.; Hartzell, C. J.; McMahon, T. J.; Drobny, G. P.; Dahlquist, F. W. *J. Am. Chem. Soc.* **1987**, *109*, 5956−5962.
(32) Teng, Q.; Iqbal, M.; Cross, T. A. *J. Am. Chem. Soc.* **1992**, *114*, 5312−5321.
(33) Lumsden, M. D.; Wasylishen, R. E.; Eichele, K.; Schindler, M.; Penner, G. H.; Power, W. P.; Curtis, R. D. *J. Am. Chem. Soc.* **1994**, *116*, 1403−1413.
(34) Asakawa, N.; Takenoiri, M.; Sato, D.; Sakurai, M.; Inoue, Y. *Magn. Reson. Chem.* **1999**, *37*, 303−311.
(35) Wei, Y.; Lee, D.-K.; Ramamoorthy, A. *J. Am. Chem. Soc.* **2001**, *123*, 6118−6126.
(36) Pang, Y.; Zuiderweg, E. R. P. *J. Am. Chem. Soc.* **2000**, *122*, 4841−4842.
(37) Cisnetti, F.; Loth, K.; Pelupessy, P.; Bodenhausen, G. *ChemPhysChem* **2004**, *5*, 807−814.
(38) Markwick, P. R. L.; Sattler, M. *J. Am. Chem. Soc.* **2004**, *126*, 11424−11425.
(39) Duncan, T. M. *A Compilation of Chemical Shift Anisotropies*; The Farragut Press: Chicago, 1990.
(40) Lee, D. K.; Wittebort, R. J.; Ramamoorthy, A. *J. Am. Chem. Soc.* **1998**, *120*, 8868−8874.
(41) Heise, B.; Leppert, J.; Ramachandran, R. *Solid State NMR* **2000**, *16*, 177−187.
(42) Fushman, D.; Cowburn, D. *J. Am. Chem. Soc.* **1998**, *120*, 7109−7110.
(43) Fushman, D.; Tjandra, N.; Cowburn, D. *J. Am. Chem. Soc.* **1998**, *120*, 10947−10952.
(44) Damberg, P.; Jarvet, J.; Gräslund, A. *J. Am. Chem. Soc.* **2005**, *127*, 1995−2005.
(45) Kroenke, C. D.; Rance, M.; Palmer, A. G., III. *J. Am. Chem. Soc.* **1999**, *121*, 10119−10125.
(46) Fushman, D.; Tjandra, N.; Cowburn, D. *J. Am. Chem. Soc.* **1999**, *121*, 8577−8582.
(47) Canet, D.; Barthe, P.; Mutzenhardt, P.; Roumestand, C. *J. Am. Chem. Soc.* **2001**, *123*, 4567−4576.
(48) Gerald, R. I.; Bernhard, T.; Haeberlen, U.; Rendell, J.; Opella, S. J. *J. Am. Chem. Soc.* **1993**, *115*, 777−782.
(49) Wu, C. H.; Ramamoorthy, A.; Gierasch, L. M.; Opella, S. J. *J. Am. Chem. Soc.* **1995**, *117*, 6148−6149.
(50) Tjandra, N.; Bax, A. *J. Am. Chem. Soc.* **1997**, *119*, 8076−8082.
(51) Tessari, M.; Vis, H.; Boelens, R.; Kaptein, R.; Vuister, G. W. *J. Am. Chem. Soc.* **1997**, *119*, 8985−8990.
(52) Sharma, Y.; Kwon, O. Y.; Brooks, B.; Tjandra, N. *J. Am. Chem. Soc.* **2002**, *124*, 327−335.
(53) Goldman, M. *J. Magn. Reson.* **1984**, *60*, 437−499.

Table 1. Rates Measured To Determine the CSA Parameters of the N, C′, and H^N Nuclei

single quantum cross-correlation rates	remote cross-correlation rates	auto-correlated relaxation rates
$R(N/NH^N)$, $R_L(N/NH^N)$, $R(N/NC')$	$R(N/C'H^N)$	$R_1(N)$
$R(H^N/H^NN)$, $R(H^N/H^NC')$	$R(H^N/NC')$	$NOE(NH^N)$
$R(C'/C'N)$, $R(C'/C'H^N)$, $R(C'/C'C^\alpha)$	$R(C'/NH^N)$	$R_1(C')$

of the spectral densities for different motional models used in this work is given in the Supporting Information. A remote CSA/DD cross-correlation rate depends only on spectral densities at zero frequency:

$$R(I/XS) = 2c_I c_{XS}[(\sigma_{xx}^{\ I} - \sigma_{zz}^{\ I})4J_{xx,XS}(0) + (\sigma_{yy}^{\ I} - \sigma_{zz}^{\ I})4J_{yy,XS}(0)] \quad (2)$$

When there are no internal motions, three cross-correlation rates per nucleus are sufficient to extract the three independent CSA parameters.[36] To take internal motions into account, we have determined a total of 10 transverse cross-correlation rates, the longitudinal cross-correlation rate $R_L(N/NH^N)$, the longitudinal auto-relaxation rates $R_1(C')$ and $R_1(N)$, and the cross-relaxation rate (NOE) between $^1H^N$ and ^{15}N. We have chosen only relaxation rates that are not sensitive to exchange phenomena. In the Supporting Information, the expressions for the auto-correlated relaxation rates are given. The single quantum cross-correlation rate $R(I/IS)$ can be determined by measuring the interconversion between the operators I_y and $2I_yS_z$.[54] A remote cross-correlation rate $R(I/XS)$ causes the interconversion between $2I_yX_y$ and $4I_xX_xS_z$. However, the "parasitic" rate $R(X/IS)$ leads to the same conversion, and its effects are indistinguishable from those of $R(I/XS)$.[55] To extract the rates $R(C'/H^NN)$, $R(H^N/C'N)$, and $R(N/H^NC')$, we have measured the rates of interconversion:

$$2C'_xH_x^{\ N} \leftrightarrow 4C'_yH_y^{\ N}N_z \quad \text{due to} \quad R(C'/H^NN) + R(H^N/C'N) \quad \text{(I)}$$

$$2H_x^{\ N}N_x \leftrightarrow 4H_y^{\ N}N_yC'_z \quad \text{due to} \quad R(H^N/C'N) + R(N/H^NC') \quad \text{(II)}$$

$$2N_xC'_x \leftrightarrow 4N_yC'_yH_z^{\ N} \quad \text{due to} \quad R(N/H^NC') + R(C'/H^NN) \quad \text{(III)}$$

Thus, the different cross-correlation rates can be obtained by:

$$2R(H^N/C'N) = \text{(I)} + \text{(II)} - \text{(III)}$$

$$2R(N/H^NC') = \text{(II)} + \text{(III)} - \text{(I)}$$

$$2R(C'/H^NN) = \text{(I)} + \text{(III)} - \text{(II)}$$

In Table 1, the different relaxation rates are listed. Cross-correlated relaxation causes the interconversion between the operators P (e.g., H_y) and Q (e.g., $2H_yN_z$). This rate can be measured by detecting the decays of P and Q and the conversion of P into Q and vice versa in four interleaved experiments.[56]

The choice of the cross-correlation experiments was based on the following criteria: both operators P and Q must be transferable into an observable amide proton coherence, the cross-correlation rates should not be overshadowed by the auto-correlated relaxation rates, and the cross-correlation rates should not to be polluted by "parasitic" rates that are difficult to separate.

Experimental Section

A sample of uniformly $^{13}C/^{15}N/^2H$ labeled human ubiquitin, a small protein with 76 amino acids (8.6 kDa), was obtained from VLI Research. The 1.5 mM sample was dissolved in H_2O/D_2O = 9:1, buffered at pH = 4.5 with 20 mM perdeuterated acetic acid, and transferred to a Shigemi tube with a volume of 150 μL. The spectra were recorded at 300 K with a Bruker Avance 600 MHz spectrometer equipped with a triple frequency probe with triple-axes pulsed field gradients. In the Supporting Information, the 10 pulse sequences used to measure the cross-correlation rates are shown.

First, the anisotropic diffusion tensor has been determined from the ratio of the transverse $R(N/NH^N)$ and longitudinal $R_L(N/NH^N)$ rates.[57] The CSA parameters of the ^{15}N nuclei and the motional parameters that determine the spectral densities were then extracted by minimizing the χ^2 of the difference between experimental and theoretical relaxation rates that involved ^{15}N. The CSA parameters of the $^{13}C'$ and $^1H^N$ nuclei were obtained by fitting them to theoretical rates, using the motional parameters derived from the ^{15}N rates.

The errors in the relaxation rates were estimated from the noise level in the experiments and evaluated by comparing the rates obtained at different relaxation times. The errors in the CSA and dynamical parameters were estimated by fitting the parameters while varying each of the relaxation rates 100 times randomly and independently by stochastic variations with a standard deviation equal to the experimental error. The final three C-terminal residues have not been taken into account when evaluating the average parameters since they suffer from large-amplitude internal motions, so that the definitions of the order parameters given in the Supporting Information do not apply.

Results and Discussion

Figure 2 shows the experimental transverse cross-correlation rates. The total experimental time was about 14 days for the measurement of all 14 auto- and cross-correlation rates. A table specifying the time required for each experiment can be found in the Supporting Information. When only the nitrogen CSA needs to be determined, the rates in the second and third rows of the left column in Table 1 and $R_1(C')$ need not be measured. For the proton CSA the rates in the third row of the left column in Table 1 and $R_1(C')$ are superfluous, while for the carbonyl CSA one can skip the rates in the second row of the left column in Table 1.

In a first approach, we assumed that internal motions of each peptide plane can be described by isotropic wobbling-in-a-cone. This means that all relaxation rates of a given peptide plane are scaled by a uniform order parameter and characterized by a single internal correlation time (see Supporting Information). In Figure 3 (top row for isotropic local motion), the principal components of the CSA tensors of the three nuclei are plotted as a function of the isotropic chemical shifts. For C′, the results of previous studies are confirmed.[31,37,38] The least (σ_{xx}) and most (σ_{zz}) shielded components are fairly constant while the σ_{yy}

(54) Tjandra, N.; Szabo, A.; Bax, A. *J. Am. Chem. Soc.* **1996**, *118*, 6986−6991.
(55) Reif, B.; Diener, A.; Hennig, M.; Maurer, M.; Griesinger, C. *J. Magn. Reson.* **2000**, *143*, 45−68.
(56) Pelupessy, P.; Espallargas, G. M.; Bodenhausen, G. *J. Magn. Reson.* **2003**, *161*, 258−264.
(57) Kroenke, C. D.; Loria, J. P.; Lee, L. K.; Rance, M.; Palmer, A. G., III. *J. Am. Chem. Soc.* **1998**, *120*, 7905−7915.

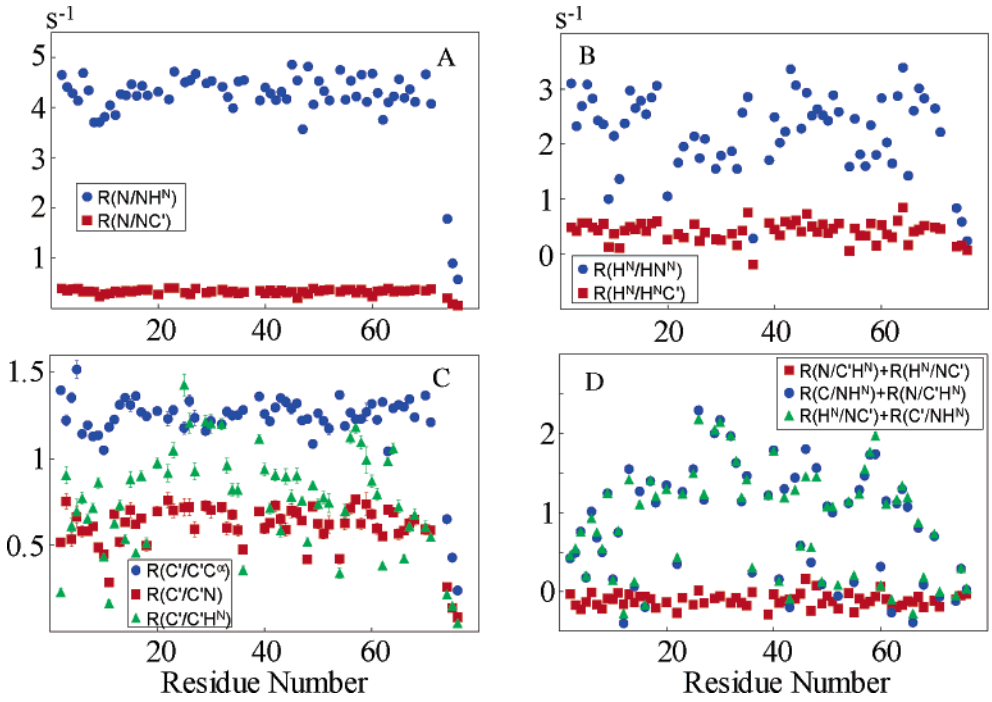

Figure 2. Experimental transverse cross-correlation rates for 64 residues in ubiquitin. (A) R(N/NH^N) and R(N/NC′), (B) R(H^N/H^{N}N) and R(H^N/H^{N}C′), (C) R(C′/C′C$^\alpha$), R(C′/C′N), and R(C′/C′H^N), (D) R(C′/H^{N}N) + R(H^N/C′N), R(H^N/C′N) + R(N/H^{N}C′), and R(N/H^{N}C′) + R(C′/H^{N}N).

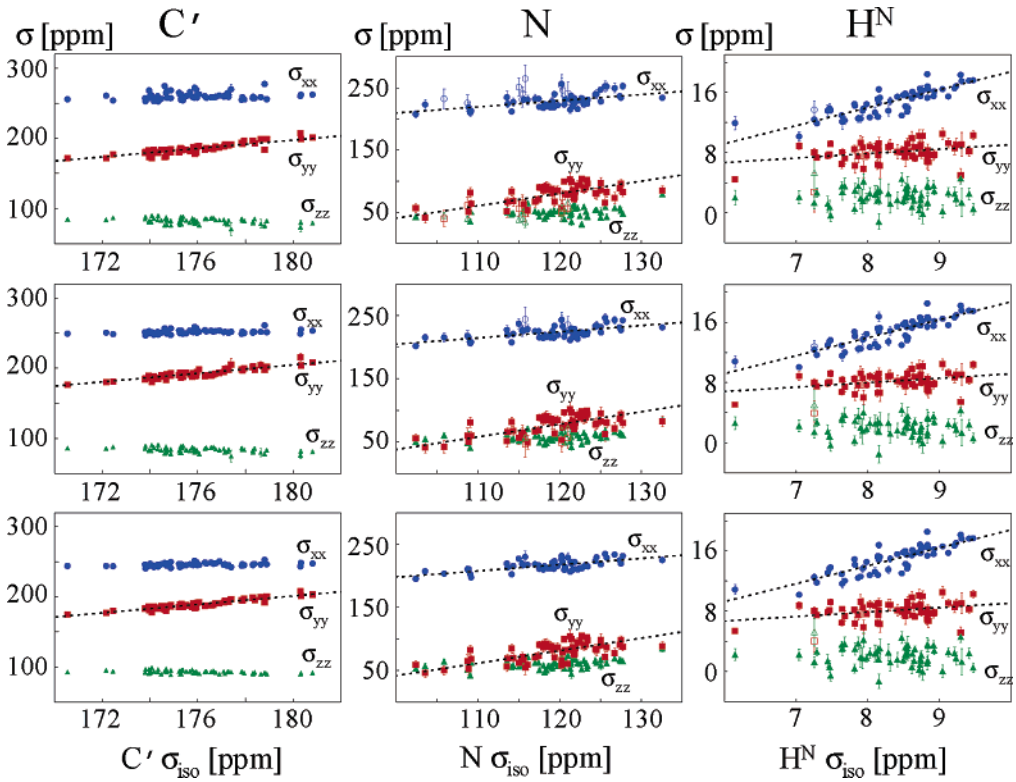

Figure 3. Principal components σ_{xx}, σ_{yy}, and σ_{zz} of the CSA tensors of the C′, N, and H^N nuclei (from left to right) for 61 residues in ubiquitin derived from the isotropic model (first row), an axially symmetric 3D-GAF model with a single internal correlation time for each residue, and a dominant motion around the C$^\alpha$C$^\alpha$ axis with an amplitude σ_γ that is twice as large as the amplitudes of the motions about the perpendicular axes ($\sigma_\gamma = 2\sigma_\alpha = 2\sigma_\beta$) (second row), and a model in which the amide proton is allowed to move out of the peptide plane separately while the remaining peptide plane wobbles around an axis parallel to the average NH bond with an internal correlation time $\tau_{pep} = 400$ ps (third row).

component that lies approximately parallel to the CO bond determines most of the variation of the isotropic shift. The orientation $\beta_{C'}$ varies from 30° to 47° (see Figure 4). Compared to our previous study,[37] the standard deviations are reduced by a factor of 2 (see Table 2). This is due to a more elaborate approach of the present study: the anisotropic overall diffusion, the time scale of the internal motions, and the effect of the variations of the nitrogen CSA tensors on the order parameters

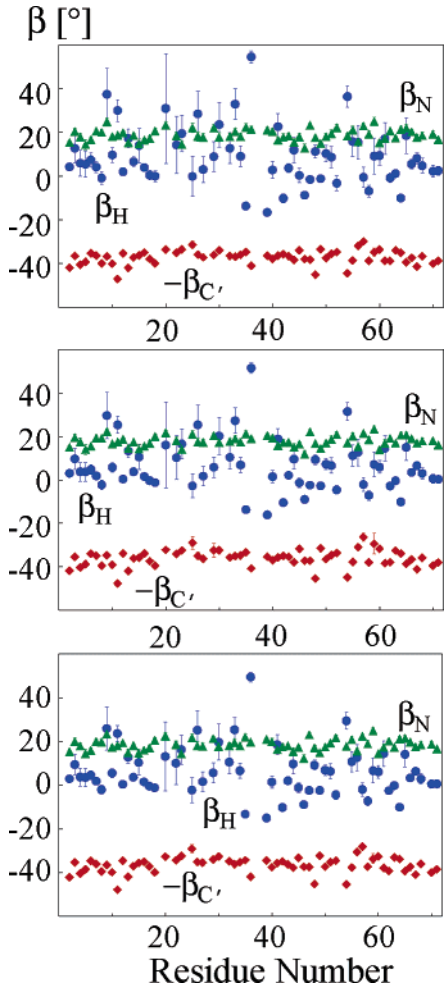

Figure 4. Orientation of the CSA tensors of the C′, N, and H^N nuclei for 61 residues in ubiquitin. Three models are considered with parameters identical to those of Figure 3. For clarity, we have multiplied the angle $\beta_{C'}$ by −1.

have been taken into account, and two additional relaxation rates have been used.

For the N nuclei, the most shielded components (σ_{zz}) do not vary much when plotted as a function of the isotropic shift. The deviation from axial symmetry as defined by the asymmetry parameter $\eta_N = |(\sigma_{yy} - \sigma_{zz})/(\sigma_{xx} - \sigma_{iso})|$ increases with the isotropic shift. The σ_{yy} component perpendicular to the peptide plane and the least shielded σ_{xx} component vary linearly with the isotropic shift: $\sigma_{xx} \approx 1.0 \times \sigma_{iso} + 109.3$ and $\sigma_{yy} \approx 2.0 \times \sigma_{iso} - 159.5$. Note that we have excluded some residues that have large errors from the linear regression. These residues are indicated by unfilled symbols. The angle β_N ranges from 12° to 25° (see Figure 4 top row for isotropic local motion). The variations of the principal components are much more pronounced for the nitrogen than for the carbonyl CSA tensor, while the dispersion of the angles β_N and $\beta_{C'}$ are comparable. The average value for η_N is 0.29, while the average value of the anisotropy, defined as $\Delta\sigma_N = \sigma_{xx} - (\sigma_{yy} + \sigma_{zz})/2$, is 164.0 ppm (see Table 2). These values fall in the range reported in the litterature.[13,39,43,45]

The tendencies for the principal components of the amide protons H^N are similar to those of the amide nitrogen nuclei: the isotropic chemical shifts show strong correlations with σ_{xx} (perpendicular to the peptide plane). A linear regression results in $\sigma_{xx} \approx 2.4 \times \sigma_{iso} - 5.2$, while σ_{yy} seems to increase slightly with the isotropic shift: $\sigma_{yy} \approx 0.6 \times \sigma_{iso} + 3.1$ (we have forced the slope to be 0.6 so that $\sigma_{xx} + \sigma_{yy} = 3.0 \times \sigma_{iso} + \text{constant}$). On the other hand, σ_{zz} (approximately parallel to the NH^N bond) is not correlated with the isotropic chemical shift. The average angle β_H is 8.9°. Since only three rates are used to fit the CSA parameters of the protons, the precision is not as good as that for the C′ and N nuclei.

Some studies suggest that the so-called three-dimensional Gaussian axial fluctuation (3D-GAF) model is more appropriate to describe the internal motions of peptide planes in proteins. In this model, the dominant motion (with an amplitude σ_γ) is assumed to be around the $C^\alpha C^\alpha$ axis, while motions around the two axes perpendicular to the $C^\alpha C^\alpha$ axis (with amplitudes σ_α and σ_β) have about half the amplitude of the dominant motion.[58] The results of a fit to an axially symmetric 3D-GAF model with $\sigma_\gamma = 2\sigma_\alpha = 2\sigma_\beta$ can be seen in the second rows of Figures 3 and 4. The tendencies are the same as those for isotropic local motion. However, the variations of the CSA tensors about the average values are less pronounced, as can be seen in the second row of Table 2. The fit of the C′ rates has, in general, a lower χ^2, suggesting that the axially symmetric 3D-GAF model fits the data better than isotropic local motion.

The validity of the 3D-GAF model is open to debate. It has been suggested that the amide proton can move independently out of the peptide plane.[59−61] We have tried a model in which the predominant motion of the entire peptide plane occurred about an axis parallel to the average position of the NH bond (with an amplitude σ_{pep}), while the amide proton has an additional out-of-the-plane motion around an axis (close to the $C^\alpha C^\alpha$ axis) lying in the peptide plane perpendicular to the average NH bond (with an amplitude σ_{NH}) as suggested by Wang et al.[61] Calculations of the CSA parameters using models with a motion of the entire peptide plane about an axis perpendicular to the peptide plane or lying in the peptide plane perpendicular to the NH bond resulted in poorer fits. The time scales of the two motions need not be identical. The correlation time of the motions that are perpendicular to the average NH bond, τ_{NH}, is determined mainly by the NOE rates. In this model, we have fitted site-specific parameters for motions perpendicular to the average NH bond (internal correlation time τ_{NH} and amplitude σ_{NH}), but we optimized average parameters for the motions of the remaining peptide planes simultaneously for all residues, otherwise the fit became unstable. The optimum average amplitude $\langle\sigma_{pep}\rangle$ of the motions of the peptide planes about the average NH bond vectors is strongly correlated with the average internal correlation time $\langle\tau_{pep}\rangle$ chosen. The third and fourth rows of Table 2 show the results for two internal correlation times. For an internal correlation time $\langle\tau_{pep}\rangle = 40$ ps (third row), the amplitude that best fitted the results was $\langle\sigma_{pep}\rangle = 14.3°$, while for an internal correlation time $\langle\tau_{pep}\rangle = 400$ ps (fourth row), this amplitude was 8.6°. The model with the largest $\langle\tau_{pep}\rangle$ seems to provide the best fit to the data (the results are shown in the bottom rows of Figures 3 and 4). However, the

(58) Lienin, S. F.; Bremi, T.; Brutscher, B.; Brüschweiler, R.; Ernst, R. R. *J. Am. Chem. Soc.* **1998**, *120*, 9870−9879.
(59) MacArthur, M. W.; Thornton, J. M. *J. Mol. Biol.* **1996**, *264*, 1180−1195.
(60) Mannfors, B. E.; Mirkin, N. G.; Palmo, K.; Krimm, S. *J. Phys. Chem. A* **2003**, *107*, 1825−1832.
(61) Wang, T. Z.; Cai, S.; Zuiderweg, E. R. P. *J. Am. Chem. Soc.* **2003**, *125*, 8639−8643.

Table 2. Principal Components σ_{xx}, σ_{yy}, σ_{zz} and Orientations β of the CSA Tensors, Asymmetry η, and Anisotropy $\Delta\sigma$ Parameters of the C′, N, and H^N Nuclei Averaged over All Available Peptides Plane in Ubiquitin

	mod[a]	$\langle\sigma_{xx}\rangle^c$ (ppm)	$\langle\sigma_{yy}\rangle^c$ (ppm)	$\langle\sigma_{zz}\rangle^c$ (ppm)	$\langle\beta\rangle^c$ (deg)	$\langle\eta\rangle^b$	$\langle\Delta\sigma\rangle^b$ (ppm)
(1)	C′	260.4 (1.5; 5.2)	$3.0 \times \sigma_{iso} - 342.9$ (0.6; 3.7)	82.1 (1.9; 4.0)	37.2 (0.8; 3.2)	0.80	−140.7
	N	$1.0 \times \sigma_{iso} + 109.3$ (5.0; 9.1)	$2.0 \times \sigma_{iso} - 159.5$ (7.4; 12.1)	50.2 (3.4; 8.1)	18.2 (1.4; 2.4)	0.29	164.0
	H^N	$2.4 \times \sigma_{iso} - 5.2$ (0.3; 1.0)	$0.6 \times \sigma_{iso} + 3.1$ (0.7; 1.1)	2.1 (0.9; 1.2)	8.9 (4.9; 13.2)	0.96	9.7
(2)	C′	251.8 (0.3; 2.7)	$3.0 \times \sigma_{iso} - 335.4$ (1.6; 3.2)	83.6 (1.6; 3.4)	36.1 (1.0; 3.9)	0.65	−138.5
	N	$1.0 \times \sigma_{iso} + 104.5$ (4.4; 7.7)	$2.0 \times \sigma_{iso} - 162.2$ (7.8; 11.9)	57.7 (3.7; 7.3)	17.6 (1.3; 2.3)	0.22	156.7
	H^N	$2.4 \times \sigma_{iso} - 5.3$ (0.3; 1.0)	$0.6 \times \sigma_{iso} + 3.2$ (0.6; 1.0)	2.1 (0.8; 1.2)	6.3 (3.7; 11.8)	0.99	9.6
(3)	C′	257.9 (0.6; 2.8)	$3.0 \times \sigma_{iso} - 337.3$ (0.8; 2.7)	79.5 (0.4; 2.4)	35.0 (0.8; 3.3)	0.70	−144.7
	N	$1.0 \times \sigma_{iso} + 98.7$ (3.4; 7.0)	$2.0 \times \sigma_{iso} - 158.0$ (7.7; 13.2)	59.3 (4.5; 8.8)	18.9 (1.3; 2.7)	0.27	148.0
	H^N	$2.4 \times \sigma_{iso} - 5.0$ (0.3; 1.0)	$0.6 \times \sigma_{iso} + 3.7$ (0.8; 1.3)	1.2 (1.0; 1.5)	7.2 (4.6; 12.6)	1.14	10.1
(4)	C′	245.9 (0.4; 2.3)	$3.0 \times \sigma_{iso} - 338.8$ (0.6; 2.5)	92.9 (0.3; 2.1)	36.5 (0.9; 3.7)	0.69	−124.6
	N	$1.0 \times \sigma_{iso} + 97.6$ (3.3; 6.8)	$2.0 \times \sigma_{iso} - 158.6$ (7.3; 11.3)	61.0 (4.2; 7.4)	18.4 (1.3; 2.6)	0.23	146.4
	H^N	$2.4 \times \sigma_{iso} - 5.2$ (0.3; 1.0)	$0.6 \times \sigma_{iso} + 3.1$ (0.6; 1.1)	2.1 (0.8; 1.2)	6.0 (3.5; 11.2)	0.96	9.7
(5)	C′	245.6 (0.6; 2.3)	$3.0 \times \sigma_{iso} - 338.5$ (0.8; 2.6)	92.8 (0.4; 2.2)	36.7 (0.9; 3.7)	0.68	−124.7
	N	$1.0 \times \sigma_{iso}$+105.8 (4.9; 8.6)	$2.0 \times \sigma_{iso} - 166.8$ (8.6; 13.2)	61.0 (4.0; 7.4)	17.5 (1.1; 2.2)	0.18	158.7
	H^N	$2.4 \times \sigma_{iso}$−5.1 (0.3; 1.0)	$0.6 \times \sigma_{iso} + 3.2$ (0.6; 1.1)	1.9 (0.8; 1.2)	6.2 (3.5; 11.2)	0.98	10.0

[a] Different models were tested: (1) Isotropic local wobbling-in-a-cone model; (2) An axially symmetric 3D-GAF model with a single internal correlation time for each residue and the dominant motion around the $C^{\alpha}C^{\alpha}$ axis with an amplitude σ_γ that is twice as large as the amplitudes of the motions about the perpendicular axes ($\sigma_\gamma = 2\sigma_\alpha = 2\sigma_\beta$); (3) Model in which the amide proton H^N is allowed to move out of the peptide plane separately while the remaining peptide plane moves around an axis parallel to the average NH^N bond with an internal correlation time $\tau_{pep} = 40$ ps; (4) same as (3) but with $\tau_{pep} = 400$ ps; (5) same as (4) but the N CSA tensor follows the motions of the NH^N bond. [b] For H^N and N, $\eta \equiv |(\sigma_{yy} - \sigma_{zz})/(\sigma_{xx} - \sigma_{iso})|$ and $\Delta\sigma \equiv \sigma_{xx} - (\sigma_{yy} + \sigma_{zz})/2$. For C′, $\eta \equiv |(\sigma_{yy} - \sigma_{xx})/(\sigma_{zz} - \sigma_{iso})|$ and $\Delta\sigma \equiv \sigma_{zz} - (\sigma_{xx} + \sigma_{yy})/2$. [c] In parentheses: average errors and standard deviations over 61 residues for C′ and over 60 residues for H^N. For N, the averages were calculated over (1) 52, (2) 58, (3) 60, (4) 61, and (5) 56 peptide planes. The errors were estimated by recalculating the tensor parameters while varying each of the relaxation rates 10^2 times randomly and independently by stochastic variations with a standard deviation equal to the experimental errors.

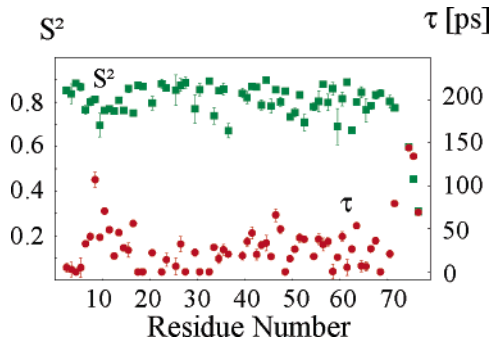

Figure 5. Dynamical order parameters S^2 (green ■) associated with the NH^N dipoles and internal correlation times τ_{int} (red ●) of 64 residues in ubiquitin, obtained from the fit of the relaxation rates that involve ^{15}N to an isotropic model of local motions.

resulting anisotropy of the nitrogen CSA tensor is very low compared to the values reported in the literature. This might be because we have assumed that the nitrogen CSA tensors do not follow the motions of the NH bonds. In the fifth row of Table 2, the results of a fit where the nitrogen CSA tensors follow the motions of the NH bonds are shown. The parameters are the same as those in the fourth row. The parameters of the carbonyl and the proton CSA tensors are hardly affected, while the nitrogen anisotropy has increased from the fourth to the fifth row of Table 2.

The dynamical parameters that result from a fit of the isotropic wobbling-in-a-cone model are plotted in Figure 5. We have drawn the internal correlation times τ_{int} and the order parameters S^2 associated with the NH^N dipoles. The values of these dynamical parameters do not change very much for our different models (see the Supporting Information). Depending on the model chosen, the order parameters S^2 shift systematically to higher or lower values. In the Supporting Information we have also plotted against each other the dynamical (Figure S14) and CSA parameters (Figure S15) obtained with different models.

Conclusions

We have determined the CSA parameters of the C′, N, and H^N nuclei in a small protein. Although the exact values of these parameters depend on the model chosen for the internal motions (note that even in solid-state NMR measurements of CSA tensors, the results can be distorted by internal motions), some general trends can be observed. For the C′ nuclei, the least and most shielded components hardly vary, while the central component, which is almost parallel to the CO bond, determines most of the variations of the isotropic chemical shift. The σ_{xx} component is tilted by about $\beta_{C'} = 36°$ from the C′N bond toward the C′O bond (see Figure 1). The dispersion about the average values is surprisingly small (about 3 ppm for the principal components and 3.5° for the orientation). These variations represent upper values of the true dispersion of the individual CSA parameters, since the latter may also be due to variations in bond angles or internuclear distances, as well as deviations from various models of internal motions.[37]

For the N nuclei, the deviation of the CSA tensors from axial symmetry increases with increasing isotropic chemical shift. There is no apparent correlation between the most shielded component and the isotropic chemical shift, whereas there is a strong correlation for the component perpendicular to the peptide plane and a weaker correlation for the σ_{xx} component which is closest to the NH bond. The latter component is tilted about 18° from the NH bond toward the C′N bond. The dispersion about the average values of the principal components is considerably larger for N than for the C′, while the variations of the orientations are similar.

For the amide protons, the tendencies for the principal components are similar to those of the amide nitrogens: the σ_{zz} component is tilted by about 7° from the NH bond toward the C′N bond and does not correlate with the isotropic shift, while the other two components do. The anisotropy of the CSA tensor increases with the isotropic shifts.

It is difficult to determine which model of internal motions is most appropriate. The axially symmetric 3D-GAF model fits the data better than the isotropic model, while the models in which the proton is allowed to move independently seem to fit even better. However, one has to be very careful, since small systematic experimental errors (which might be due to small temperature variations between experiments), deviations of the bond lengths and angles from standard values, or errors in the global structure (obtained by NMR[62]) might tilt the balance toward one motional model rather than another. The most realistic model might be an intermediate between the models presented in this work. Nevertheless, one can conclude that while the amplitudes of the internal motions vary from residue to residue, the fast internal motions in ubiquitin appear to be surprisingly uniform, except for the three C-terminal residues. The differences between the average values of the carbonyl CSA parameters determined using different models exceed the standard deviations. If, using the 3D-GAF model, the variations of these parameters were *entirely* due to variations of the ratio ζ between the amplitudes of the motions about axes that are perpendicular and parallel to the $C^{\alpha}C^{\alpha}$ vector, $\sigma_{\gamma} = \zeta\sigma_{\alpha} = \zeta\sigma_{\beta}$, these variations could be explained by a ratio $\zeta = 2 \pm 0.6$. For liquid state NMR, the parameters obtained in this work can be used as effective values provided one uses a consistent motional model.

(62) Cornilescu, G.; Marquardt, J. L.; Ottiger, M.; Bax, A. *J. Am. Chem. Soc.* **1998**, *120*, 6836−6837.

Acknowledgment. This work was supported by the Centre National de la Recherche Scientifique, the European Union through the Research Training Network 'Cross-Correlation' HPRN-CT-2000-00092, a fellowship of the Ministère Délégué à la Recherche et aux Nouvelles Technologies to K.L., and the Commission pour la Technologie et l'Innovation (CTI), Switzerland.

Supporting Information Available: Figures of the 10 pulse sequences used to measure the cross-correlated relaxation rates. One figure showing the dynamical parameters τ_{int} and S^2 obtained from fits to different models used in this work, and two figures showing the CSA parameters of the two models that are not shown in Figures 3 and 4. Two figures with the dynamical and CSA parameters obtained with different models plotted against each other. One table lists the experiments performed with their duration, the number of repetitions, and the operators involved. One table lists the global and residue-specific parameters that have been fitted for the different dynamical models. Six tables list the experimental rates obtained, the principal components of the CSA tensors, and the dynamical parameters calculated for each model. Equations for the spectral densities and auto-correlated relaxation rates are also given. This material is available free of charge via the Internet at http://pubs.acs.org.

JA042863O